Available online at www.sciencedirect.com
SCIENCE DIRECT®
Journal of Nuclear Materials 343 (2005) 253–261
journal of nuclear materials
www.elsevier.com/locate/jnucmat

Tensile properties of austenitic stainless steels irradiated at SINQ target 3

S. Saito [a,*], K. Kikuchi [a], K. Usami [a], A. Ishikawa [a], Y. Nishino [a], M. Kawai [b], Y. Dai [c]

[a] JAERI Tokai, 2-4 Shirakata-shirane, Tokai-mura, Naka-gun, Ibaraki-ken 319-1195, Japan
[b] KEK, Tsukuba-shi, Ibaraki-ken 305-0801, Japan
[c] PSI, 5232 Villigen PSI, Switzerland

Abstract

The beam window of the spallation target will be subjected to proton/neutron irradiation. It is important to know the irradiation effect on structural materials to facilitate the facility design and the lifetime evaluation. The SINQ target irradiation program (STIP) at the Paul Scherrer Institute (PSI) began to obtain high-energy proton irradiation data. JAERI joined this program and shares the post irradiation experimental (PIE) work. The JAERI specimens were irradiated at 90–380 °C and dpa ranged from 3.5 to 11.8 dpa. Tensile tests were done in air at RT and 250 °C. The results on JPCA-SA and 316F-SA indicate that the irradiation caused considerable hardening and degradation of ductility. However, no drastic change of tensile properties was shown in comparison with specimens irradiated in fission reactors. Fracture surfaces were observed by microscope and their morphology revealed fracture in a ductile manner.

1. Introduction

In several institutes, research and development for an accelerator-driven spallation neutron source has been undertaken. Japan atomic energy research institute (JAERI) has planned to build two facilities with spallation neutron sources in the Japan proton accelerator complex (J-PARC) [1,2]. They are a neutron scattering facility for life and material science and a target experimental facility (TEF) for accelerator driven system (ADS) research. A spallation neutron source is composed of a high-intense proton accelerator and a heavy metal spallation target. High-flux fast neutrons are generated by a spallation reaction of high-energy protons and heavy metals. The neutrons will be used for neutron scattering research and nuclear transmutation of minor actinides (MA) in nuclear waste from atomic power plant.

Heavy liquid metals (mercury, lead-bismuth, etc.) are promising candidates for the target materials for a spallation neutron source. The beam window for the liquid metal target is subjected to proton/neutron irradiation. High-energy proton irradiation is characterized by high gas production rates and high displacement energy. It is important to know the irradiation effects on structural materials available to the facility design and the lifetime evaluation. To obtain the irradiation data, the SINQ target irradiation program (STIP) [3] at the SINQ target in Paul Scherrer Institute (PSI) was initiated in 1996 and has been progressing. JAERI joined STIP and

* Corresponding author. Tel.: +81 29 282 6426; fax: +81 29 282 6712
E-mail address: sai@popsvr.tokai.jaeri.go.jp (S. Saito).

0022-3115/$ - see front matter © 2005 Elsevier B.V. All rights reserved.
doi:10.1016/j.jnucmat.2005.02.010

conducted the post irradiation examination of Japanese Primary Candidate Alloy (JPCA), 316F-SS and F82H. Examination covers tensile tests, bending fatigue tests, hardness tests, scanning electron microscope (SEM) observation of fracture surface, metallurgical observation of microstructure after failure and measurement of gas production. Our interest is to characterize the effect of proton and neutron radiation on mechanical properties. In this study the results of tensile tests on JPCA-SA, 316F-SA and 316-F-CW are stated and compared with other data from materials irradiated in spallation and fission neutron fluxes.

2. Experimental

2.1. Materials

The chemical compositions of JPCA and 316F-SS are listed in Table 1. JPCA is a modified stainless steel by the addition of Ti to AISI type 316-SS in order to improve a swelling resistance. SA (solution-annealed) specimens were cut from 15 mm thick plates by EDM (electrical discharge machining) and mechanically polished. After polishing, JPCA and 316F specimens were solution-annealed at 1120 °C for 1 h and 1060 °C for 1 h, respectively. Some of the 316F 15 mm thick plates were solution-annealed at 1060 °C for 15 min and followed by 20% cold-work (CW). 316F-CW specimens were cut from the plates by EDM and polished. The small tensile specimen used in this study is shown in Fig. 1.

2.2. Irradiation and post irradiation experiments

The 590 MeV proton irradiation was performed at SINQ-target 3 at the PSI. The irradiation temperature ranged from 90 °C to 380 °C. The damage level ranges from 3.5 to 11.8 dpa. Calculated helium and hydrogen production rates in steels are about 70 appm/dpa and 500 appm/dpa, respectively. Details of the irradiation have been reported by Dai et al. [3,4].

Irradiation conditions of JAERI specimens are summarized in Table 2. The post irradiation experiments were performed at the Hot Laboratory at JAERI.

Tensile testing was performed in a screw driven type tensile machine. The machine was developed for the remote handling test in the hot cell. Specimens were strained at an initial rate of 6×10^{-4}/s from the both sides and to be kept almost at the same place during the loading. Strains were measured by image analyses. CCD camera and computer system were used for memorizing absolute coordinates of specimen marked as the boundary of colored area in the rectangular window and updating new window. Strains were calculated by the displacement of window between two points on the gauge part of the specimens. Tensile tests were carried out at room temperature (RT) and 250 °C in the air. A focused infrared ray heated specimens.

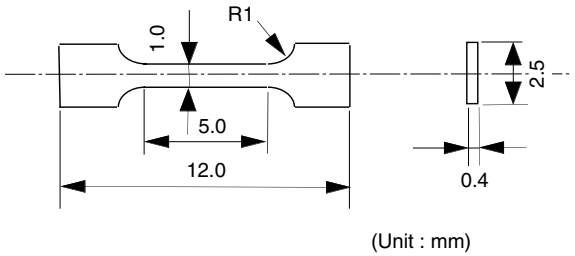

Fig. 1. Tensile specimen.

The fracture surfaces after tensile tests were observed by SEM. SHIMADZU EPM-810Q was used for the secondary electron beam image acquisition with 20 kV of accelerating voltage.

3. Results

3.1. JPCA-SA and 316F-SA

3.1.1. RT testing

Tensile properties of unirradiated and irradiated JPCA-SA and 316F-SA are summarized in Tables 2 and 3, respectively. The stress–strain curves of JPCA-SA were reported by Kikuchi et al. [5]. The selected stress–strain curves of 316F-SA tested at RT are shown in Fig. 2(a). In these plots strains were calculated by engineering definition. The results indicate that several dpa irradiation caused considerable irradiation hardening and reduction of ductility. The appearance of a stress drop after yielding is a typical phenomenon for low temperature (<300 °C) irradiation of an austenitic steel [6]. Instead of 0.2% yield strength (YS), stress peak is defined as yield strength for irradiated specimens in this paper.

Table 1
Chemical composition of JPCA and 316F

wt%	Fe	Cr	Ni	Mo	Mn	Ti	Co	B	C	Si	P	S	N
JPCA	Bal.	14.14	15.87	2.29	1.54	0.22	0.028	0.004	0.058	0.5	0.026	0.004	0.003
316F	Bal.	16.79	13.95	2.34	0.23	–	<0.01	–	0.040	0.04	<0.003	0.002	0.011

Table 2
Tensile properties of the unirradiated and the irradiated JPCA-SA specimens

ID	Tirr. (°C)	dpa	He (appm)	H (appm)	Ttest (°C)	YS (MPa)	UTS (MPa)	UE (%)	TE (%)	RA (%)	True strain to plastic instability
JPCA-SA											
AS28	–	0			23	288	528	54.4	62.4		0.294
AS30	–	0			21	214	492	45.0	52.1		
F13	–	0			25	237	501	52.7	61.6	80.6	
F5	140–160	5.7	410	2907	25	763	779	8.2	17.7	75.6	0.062
F2	210–250	7.9	569	4029	25	818	829	0.9	15.4	68.8	0.043
F11	210–240	9.1	655	4641	23	816	834	0.9	14.8		0.053
F9	260–310	10.1	727	5151	23	807	824	1.8	10.1	66.4	0.031
F8	320–380	11.8	850	6018	22	801	821	4.9	16.1		0.050
AS24	–	0			250	182	385	30.0	37.0		0.317
AS29	–	0			250	226	461	31.2	37.7	74.4	
F12	140–170	5.7	410	2907	250	543	567	12.1	17.2	81.0	0.070
F7	210–250	7.9	569	4029	250	625	625	0.2	9.7	75.7	0.032
F10	276–325	10.1	727	5151	250	690	690	0.2	7.4	69.5	0.008

Table 3
Tensile properties of the unirradiated and the irradiated 316F-SA specimens

ID	Tirr. (°C)	dpa	He (appm)	H (appm)	Ttest (°C)	YS (MPa)	UTS (MPa)	UE (%)	TE (%)	RA (%)	True strain to plastic instability
316F-SA											
G12	–	0			24	241	552	66.8	74.3	86.3	
G19	–	0			24	220	533	60.2	67.3		
G16	90–110	3.5	252	1785	27	669	669	0.1	21.0	84.5	0.055
G13	120–135	4.6	331	2346	26	681	681	0.1	28.7		0.079
G11	140–160	5.5	396	2805	26	677	680	0.3	22.0		0.066
G07	140–160	5.7	410	2907	26	689	689	0.1	19.4	87.5	0.057
G10	170–190	6.1	439	3111	25	676	676	1.1	18.3		0.052
G04	260–310	10.1	727	5151	27	723	723	0	18.8	80.9	0.051
G14	–	0			250	176	439	32.9	41.3		
G22	–	0			250	168	405	33.4	40.0	92.2	
G24	90–110	3.5	252	1785	250	487	487	4.8	19.4	87.8	0.065
G21	120–135	4.6	331	2346	250	502	502	0.1	14.1		0.041
G17	140–160	5.5	396	2805	250	520	520	0	11.2		0.024
G08	140–160	5.7	410	2907	250	531	531	0.1	10.3	91.1	0.028
G15	170–190	6.1	439	3111	250	539	539	0.1	13.3		0.040
G06	260–310	10.1	727	5151	250	577	577	0.2	10.9	81.2	0.017

At RT, YS of JPCA-SA and 316F-SA increased significantly by irradiation. Hardening of JPCA-SA almost saturates up to 10 dpa, however, hardening of 316F-SA does not saturate up to 10.1 dpa.

Uniform elongation (UE) of JPCA-SA reduced with increasing dpa. After 5.7 dpa irradiation, UE decreased to 8%. UE fell into 1–2% by over 7.8 dpa irradiation. In case of 316F-SA, UE fell into under 1% after only 3.5 dpa irradiation. Reduction of UE occurred at lower dose level compared to JPCA-SA. Sometimes UE is used to discuss a ductility of irradiated materials. UE is defined as an elongation where a load takes its maximum value. However, in cases where strain-hardening is small or almost zero, UE falls into very low values in spite of still retaining large total elongation (TE) and large reduction of area (RA). Considere's criterion [7] is applied to determine the true strain to plastic instability or necking. We discuss ductility by means of the true strain to plastic instability. The true strain to plastic instability of 316F-SA and JPCA-SA are listed in Tables 2 and 3, respectively. The true strain to plastic instability of JPCA-SA and 316F-SA ranged from 0.031 to 0.062 and from 0.051 to 0.079, respectively. In spite of very low UE values, some degree of ductility is retained.

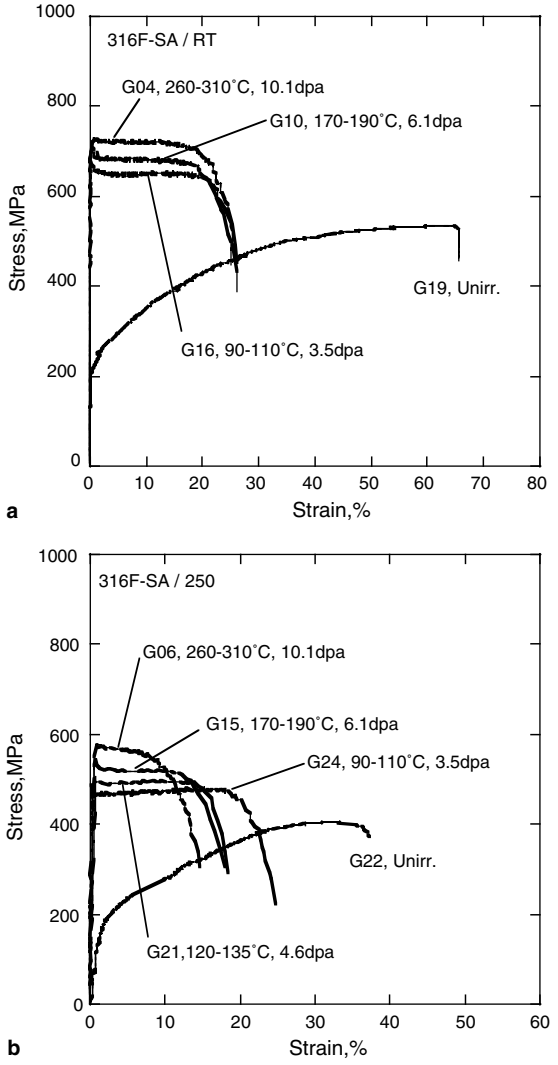

Fig. 2. Stress strain curves of the unirradiated and the irradiated 316F-SA tested at (a) RT and (b) 250 °C.

3.1.2. 250 °C testing

The selected stress–strain curves of JPCA-SA tested at 250 °C were reported by Kikuchi et al. [5]. The selected stress–strain curves of 316F-SA tested at 250 °C are shown in Fig. 2(b). At 250 °C YS of JPCA-SA and 316F-SA increased with increasing dpa and did not saturate up to 10.1 dpa.

Uniform elongation (UE) of JPCA-SA reduced with increasing dpa. After 5.7 dpa irradiation UE decreased to 12%. After 7.9 dpa and 10.1 dpa irradiation UE fell to 0.2%. Significant reduction of UE was observed at 250 °C as well as RT. In case of 316F-SA, after 3.5 dpa irradiation, UE decreased to 4.8%. After 4.6 dpa irradiation UE fell to under 0.2%. Reduction of UE occurred at a lower dpa compared to JPCA-SA as observed at room temperature. Table 3 shows the true strain to plastic instability of the irradiated specimens. It is clearly seen that the true strain to plastic instability decreased with increasing dpa. Though the decrease of ductility of 316F-SA occurred at lower dpa compared to JPCA-SA, the true strain to plastic instability of 316F-SA at higher dpa are larger than those of JPCA-SA.

3.1.3. Macro and metallographic observation

Fig. 3(a) shows the macro photographs of JPCA-SA specimens tested at 250 °C. Large plastic deformation occurred over the whole gauge section for the unirradiated specimen and low dose specimen (F12). In the engineering stress–strain curves of these specimens, the strain-hardening is observed as shown in Fig. 2(a). In case of higher dose specimens (F7, F10), small plastic

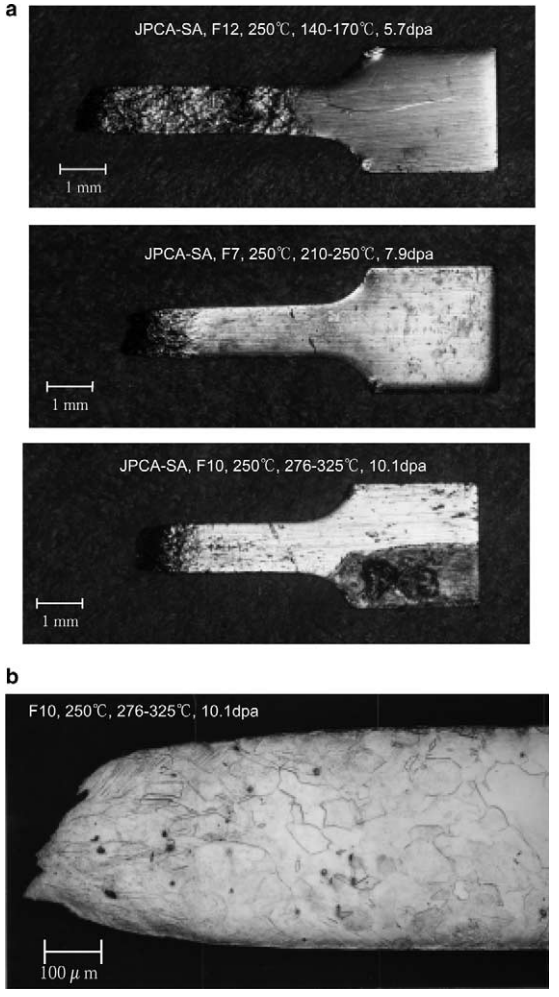

Fig. 3. (a) Macro photographs of the specimens of JPCA-SA tested at 250 °C and (b) metallographic observation of JPCA-SA tested at 250 °C.

deformation occurred before the necking. The metallographic observation of the higher dose specimen (F10) is shown in Fig. 3(b). Slip lines are clearly seen around the necking zone. These figures display that the strain localization occurred for higher dose specimens and decreased uniform elongation.

3.1.4. Fracture surface

Figs. 4 and 5 show the SEM photographs of fracture surfaces of 316F-SA tested at RT and 250 °C, respectively. Similar to JPCA-SA [5], the morphology of the fracture surface changed after irradiation. Typical dimple patterns were observed in unirradiated specimens. Elongated small dimples were observed in irradiated specimens. In any case, specimens fractured in a ductile manner. Reduction of areas (RA) is larger than that of irradiated JPCA-SA specimens. Especially, RA on the specimens tested at 250 °C are almost the same as unirradiated specimens. The morphology of the specimens was almost chisel edge fracture.

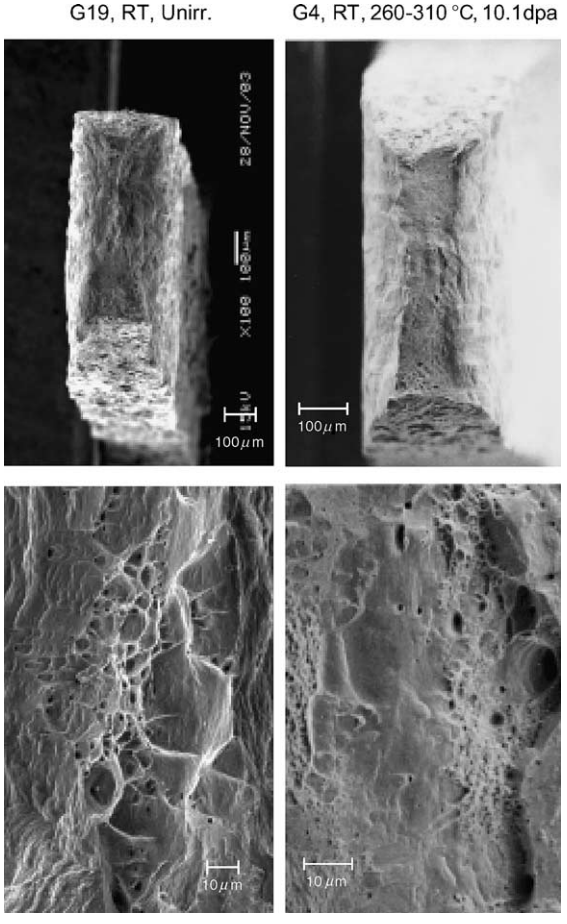

Fig. 4. Fracture surface of the unirradiated and the irradiated 316F-SA tested at RT.

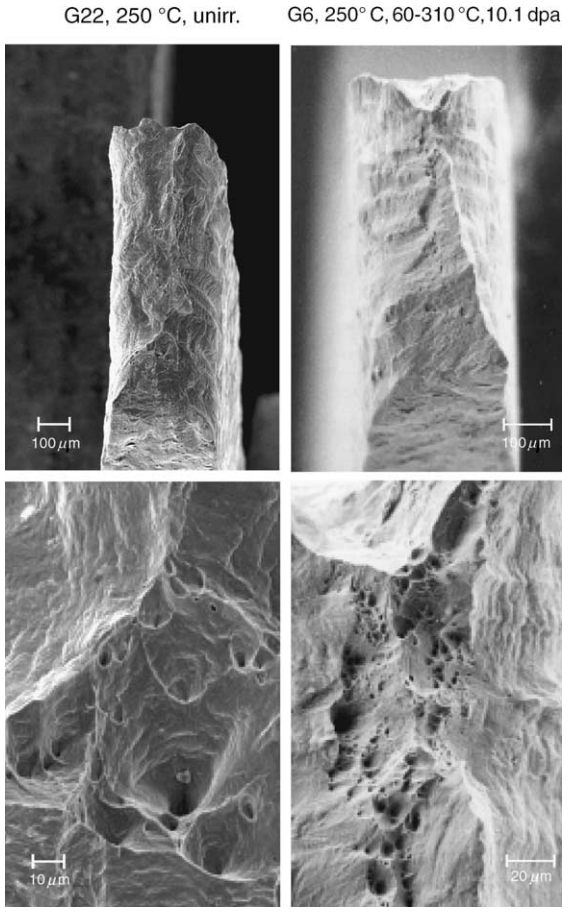

Fig. 5. Fracture surface of the unirradiated and the irradiated 316F-SA tested at 250 °C.

As shown in Table 2, RA of JPCA-SA are reduced with increasing dpa at RT. At 250 °C, RA of JPCA-SA increased by irradiation and are reduced with increasing dpa. As shown in Table 3, RA of 316F-SA does not change by irradiation up to 5.7 dpa at RT and 250 °C. After 10.1 dpa irradiation, RA of 316F-SA decreased to 10%.

3.2. 316F-CW

The tensile properties on 316F-CW are summarized in Table 4. Fig. 6(a) and (b) show the stress–strain curves tested at RT and 250 °C, respectively.

At RT unirradiated specimen had a YS of 680 MPa. YS increased slightly with increasing dpa. Hardening almost saturated up to 7.9 dpa and YS increased to about 770 MPa. Unirradiated specimens had a large UE around 20%. After 5.9 dpa irradiation strain-hardening disappeared and UE decreased to under 1%. As shown in Table 4, the true strain to plastic instability of the irradiated specimens ranged from 0.014 to 0.028.

Table 4
Tensile properties of the unirradiated and the irradiated 316F-CW specimens

ID	Tirr. (°C)	dpa	He (appm)	H (appm)	Ttest (°C)	YS (MPa)	UTS (MPa)	UE (%)	TE (%)	RA (%)	True strain to plastic instability
316F-CW											
H14	–	0			24	683	739	20.2	32.1	83.6	
H07	135–160	5.9	425	3009	26	765	768	0.5	13.6	79.1	0.022
H05	190–230	7.6	547	3876	26	777	789	0.7	10.1	83.7	0.014
H03	240–290	10.0	720	5100	25	756	778	1.5	10.6	83.9	0.028
H15	–	0			250	540	569	1.6	9.1	87.5	
H12	135–160	5.9	425	3009	250	623	623	0.2	6.4	87.1	
H10	190–230	7.6	547	3876	250	655	655	0.2	6.8	80.1	
H09	240–290	10.0	720	5100	250	645	645	0.3	6.8	74.7	
H01	310–360	11.3	814	5763	250	667	667	0.3	7.9		

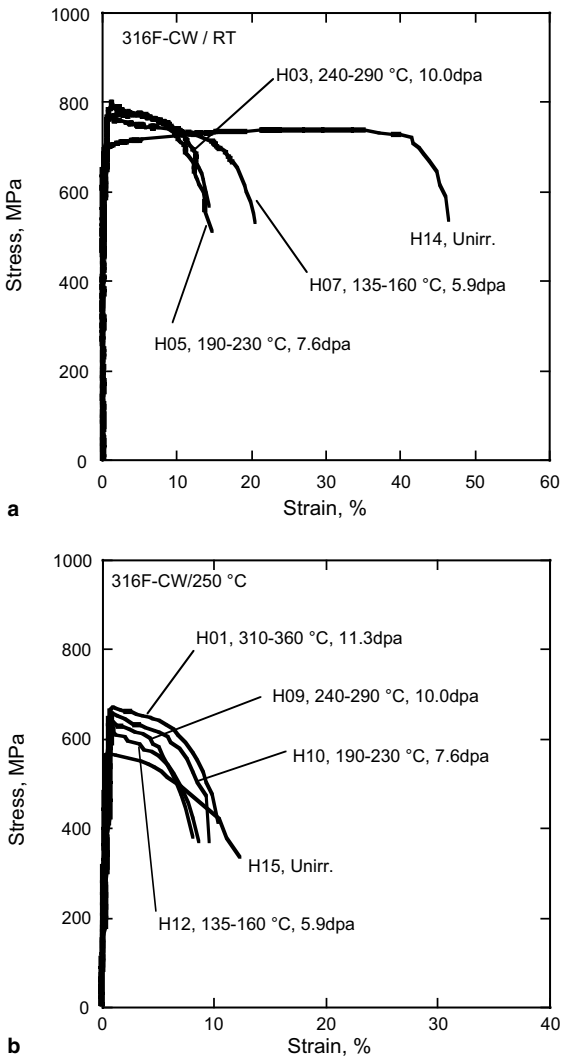

Fig. 6. Stress strain curves of the unirradiated and the irradiated 316F-CW tested at (a) RT and (b) 250 °C.

At 250 °C unirradiated specimen had a YS of about 540 MPa. YS increased to 620–670 MPa with increasing dpa and did not saturate. Unirradiated specimen had a UE of 1.6%. After 5.9 dpa of irradiation dose, UE decreased to 0.2–0.3% as shown in Table 4. The true strain to plastic instability was not able to estimate for the irra-

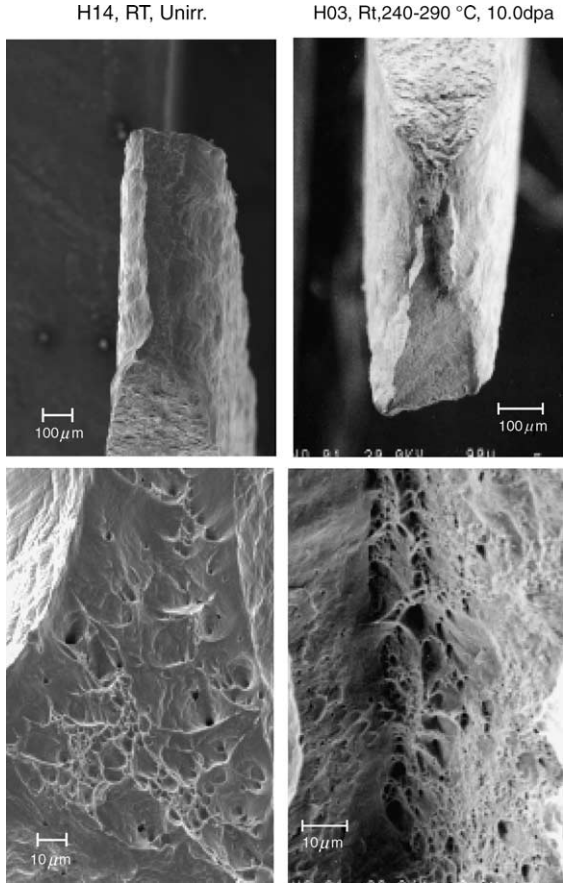

Fig. 7. Fracture surface of the unirradiated and the irradiated 316F-CW tested at RT.

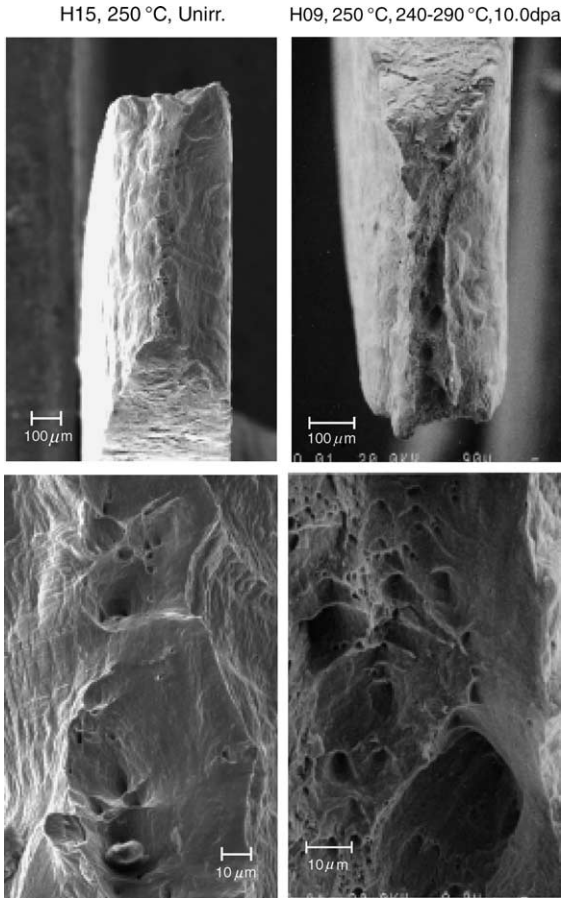

Fig. 8. Fracture surface of the unirradiated and the irradiated 316F-CW at 250 °C.

diated specimens. The results show small ductility of both the unirradiated and the irradiated 316F-CW at 250 °C.

Figs. 7 and 8 present the SEM photographs of the fracture surface of 316F-CW tested at RT and 250 °C, respectively. No significant change was observed in morphology of fracture surface after irradiation. Typical dimple patterns were observed in both unirradiated and irradiated specimens. Reduction of area of unirradiated and irradiated specimens is almost the same.

4. Discussion

The tensile properties of the proton irradiated solution-annealed austenitic stainless steels [8–12] are plotted in Figs. 9 and 10 overlaid on data bands for fission neutron irradiated ones. Irradiation and test temperature of the data were below 250 °C. Fig. 9 shows the relationship between dpa and the increase in YS. It has been reported [13,14] that the increase in YS of the fission

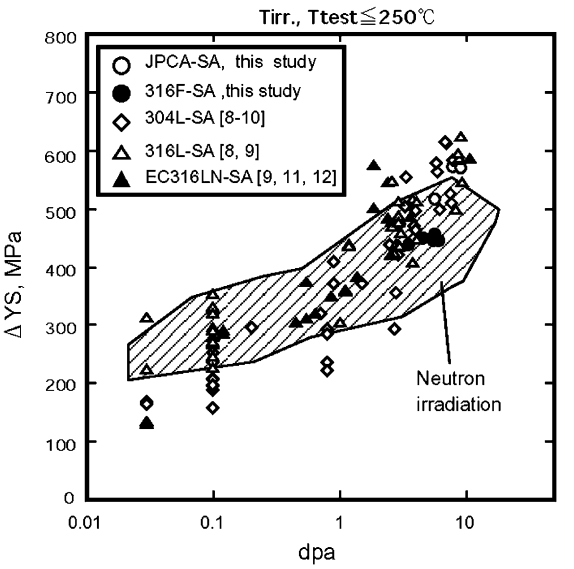

Fig. 9. The dpa dependence of increase in yield strength of proton and neutron irradiated austenitic stainless steels. (Tirr., Ttest ≦ 250 °C, and Ttest ≦ Tirr.)

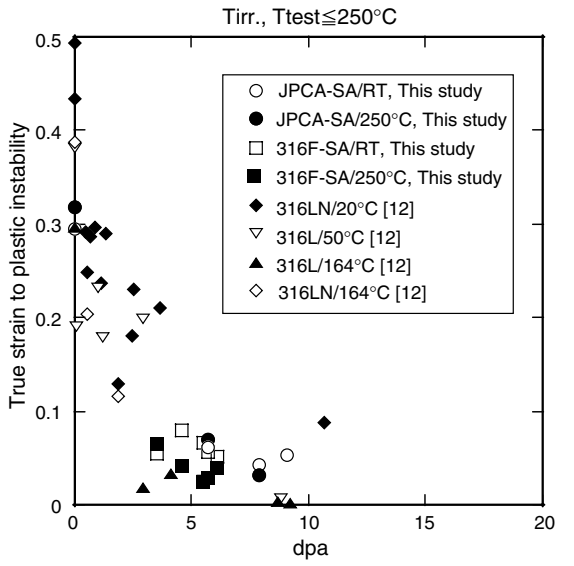

Fig. 10. The dpa dependence of the true strain to plastic instability of proton irradiated austenitic stainless steels (Tirr., Ttest ≦ 250 °C, and Ttest ≦ Tirr).

neutron irradiation is proportional to dpa to one-half power and saturates at certain dpa. The increase in YS of the proton irradiation is within the fission neutron data band at lower dose (<1 dpa). At higher dose, the YS increase does not saturate up to 10 dpa. The YS increase shows a tendency to exceed the upper bound of the fission neutron data band. The extra hardening of LANSCE irradiated materials and JPCA-SA may be

caused by the large amount of helium and hydrogen atoms and their mutual interaction. However, the increase in YS of 316F-SA are still within the fission neutron data band up to 7.6 dpa.

Fig. 10 shows the relationship between dpa and the true strain to plastic instability. JPCA-SA and 316F-SA in this study and the LANSCE data tested at 20 °C kept their ductility even near 10 dpa. In the LANSCE database [12], 316L stainless steels tested at 50 °C and 164 °C lose ductility described by the true strain to plastic instability near 10 dpa. The reason of the difference is not yet understood.

Fig. 11 shows relationships between dpa and the tensile properties on irradiated cold-worked austenitic stainless steels. Irradiation and test temperatures of the data were below 250 °C. Fig. 11 shows dpa dependence of the (a) YS and (b) UE of this study and literature values irradiated at fission reactors [15–17]. Increase of the YS is lower band of the fission database up to 10 dpa. Decrease of the UE behaves the same manner with the fission database. UE falls into almost zero by several dpa irradiation.

The results of this study show no drastic change of tensile properties in comparison with those from specimens irradiated at fission reactors. However, some results indicate that extra hardening or loss of ductility may have occurred at higher dose levels. Further investigation for specimens irradiated at higher dose levels will be needed.

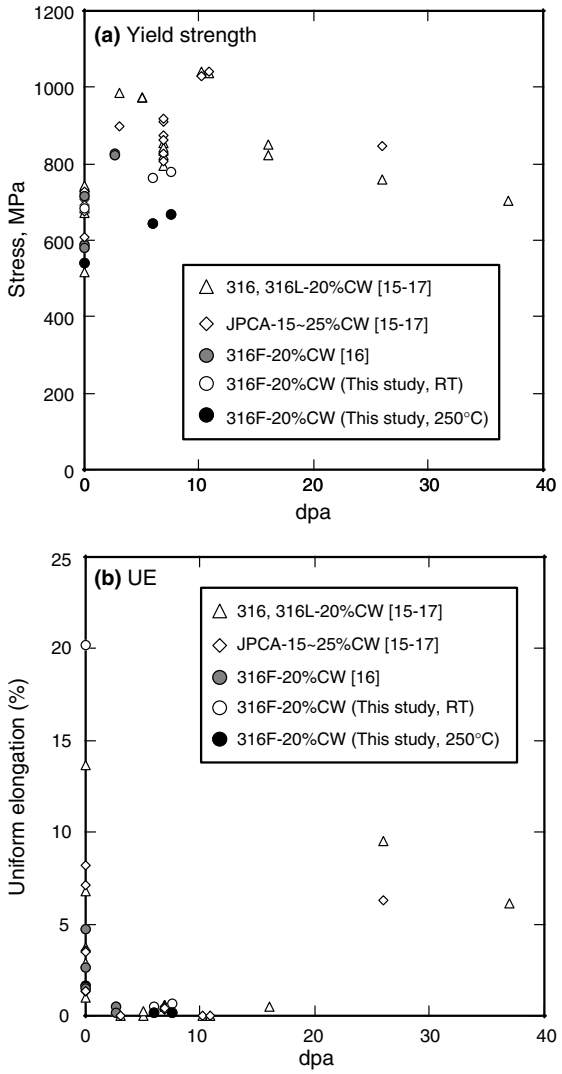

Fig. 11. The dpa dependence of yield strength and uniform elongation of cold-worked 316 series stainless steels. (Tirr., Ttest ≦ 250 °C, and Ttest ≦ Tirr.)

5. Conclusions

The tensile properties on high energy proton and spallation neutron irradiated austenitic stainless steels at 3.5–11.8 dpa were investigated. The results obtained from this study are as follows:

(1) Proton/neutron irradiation caused considerable irradiation hardening and degradation of ductility for JPCA-SA and 316F-SA. The increase in YS of irradiated specimens is within the fission neutron data band at lower dose. At higher dose, the increase in YS of JPCA-SA shows a tendency to exceed the upper bound of the fission neutron data band.
(2) Because of strain localization, UE falls to very low values in spite of large total elongation and large reduction of area. By means of the true strain to plastic instability, it was shown that the irradiated specimens still have ductility.
(3) The morphology of the fracture surface changed after irradiation. Typical dimple patterns were observed in unirradiated specimens but these were not clearly seen in irradiated ones.
(4) Proton/neutron irradiation caused a little irradiation hardening and degradation of ductility for 316F-CW. The YS values are on the lower band of the fission neutron data.
(5) The UE of 316F-CW falls to almost zero after several dpa irradiation. At RT, the true strain to plastic instability ranged from 0.014 to 0.028 for the irradiated specimens. At 250 °C, both the unirradiated and the irradiated 316F-CW show small ductility.
(6) No remarkable change was observed for 316F-CW in morphology of fracture surface after tensile tests. Typical dimple patterns were observed in both unirradiated and irradiated specimens. RA of unirradiated and irradiated specimens are almost the same.

Acknowledgment

We greatly appreciate the helpful comments and supports given by the members of Hot Laboratory during this study.

References

[1] The joint project team of JAERI and KEK, JAERI-Tech 99-056, KEK Report 99-4, JHF-99-3, 1999.
[2] Y. Oyama, JAERI-KEK Joint Project Team, ICANS-XVI, Dusseldorf-Neuss, Germany, 12–15 May 2003.
[3] Y. Dai, G.S. Bauer, J. Nucl. Mater. 296 (2001) 43.
[4] Y. Dai, Y. Foucher, M.R. James, B.M. Oliver, J. Nucl. Mater. 318 (2003) 167.
[5] K. Kikuchi, S. Saito, Y. Nishino, K. Usami, in: Proceeding of Accelerator Applications in a Nuclear Renaissance (AccApp'03), San Diego, California, June, 2003, p. 874.
[6] H.R. Higgy, F.H. Hammad, J. Nucl. Mater. 55 (1975) 177.
[7] G.E. Dieter, Mechanical Metallurgy, 289, McGraw-Hill, New York, 1986.
[8] S.A. Maloy, M.R. James, G. Willcut, W.F. Sommer, M. Solokov, L.L. Snead, M.L. Hamilton, F. Garner, J. Nucl. Mater. 296 (2001) 119.
[9] S.A. Maloy, M.R. James, W.R. Johnson, T.S. Byun, K. Farrell, M.B. Toloczko, J. Nucl. Mater. 318 (2003) 283.
[10] Y. Dai, X. Jia, J.C. Chen, W.F. Sommer, M. Victoria, G.S. Bauer, J. Nucl. Mater. 296 (2001) 174.
[11] K. Farrell, T.S. Byun, J. Nucl. Mater. 296 (2001) 129.
[12] T.S. Byun, K. Farrell, E.H. Lee, L.K. Mansur, S.A. Maloy, M.R. James, W.R. Johnson, J. Nucl. Mater. 303 (2002) 34.
[13] R.R. Vandervoot, E.L. Raymond, C.J. Echer, Rad. Eff. 45 (1980) 191.
[14] N. Yoshida, H.L. Heinisch, T. Muroga, K. Araki, M. Kiritani, J. Nucl. Mater. 179–181 (1991) 1078.
[15] S. Jitsukawa, P.J. Matiasz, T. Ishiyama, L.T. Gibson, A. Hishinumay, J. Nucl. Mater. 191–194 (1992) 771.
[16] K. Shiba, private communication.
[17] J.D. Elen, P. Fenici, J. Nucl. Mater. 191–194 (1992) 766.